

## SWIFT-XRT-CALDB-04

Release Date: December 01<sup>st</sup>, 2005

Prepared by: David Morris

Date Revised: 01 December 2005

Revision 5.0

Revised by: David Morris

Pages Changed: all



# SWIFT XRT CALDB REV 5.0 RELEASE NOTE

## SWIFT-XRT-CALDB-04: Gain

### 1. Component Files:

FILENAME	VALID DATE	RELEASE DATE	CAL VERSION
swxpcgain20010101v003.fits	1-Jan-2001	15-Oct-2004	003
swxpdgain20010101v003.fits	1-Jan-2001	15-Oct-2004	003
swxwtgain20010101v003.fits	1-Jan-2001	15-Oct-2004	003
swxpcgain20010101v005.fits	1-Sep-2005	12-Oct-2005	004
swxpdgain20010101v005.fits	1-Sep-2005	12-Oct-2005	004
swxwtgain20010101v005.fits	1-Sep-2005	12-Oct-2005	004
swxpcgain20010101v006.fits	1-Sep-2005	1-Dec-2005	005
swxpdgain20010101v006.fits	1-Sep-2005	1-Dec-2005	005
swxwtgain20010101v006.fits	1-Sep-2005	1-Dec-2005	005

### 2. Scope of Document:

This document contains a description of the gain calibration analysis performed at Penn State to produce the gain calibration products for the XRT Calibration Database.

### 3. Changes:

Temperature dependent gain:

The Gain Calibration CALDB product format has been changed to specify the gain as a function of XRT CCD temperature. In the old format of the Gain CALDB product the gain was specified as :

$$PI = ((PHA*(GC0 + x*GC1 + y*GC2) + GC3 + x*GC4 + y*GC5)/G)$$

where PI is the pulse invariant bin, PHA is the pulse height amplitude, x/y is the detector x/y coordinate of the event, G is a global PHA to PI gain factor (equal to 10) and the 6 coefficients are as follows:

- GC0: multiplicative DN to PHA gain factor
- GC1: multiplicative serial CTI correction factor
- GC2: multiplicative parallel CTI correction factor
- GC3: additive DN to PHA correction
- GC4: additive serial CTI correction
- GC5: additive parallel CTI correction

In the updated version of the Gain CALDB product the gain is now specified using an equation similar to the one above at 3 different XRT CCD temperatures, -100C, -65C and -48C. To determine the actual gain factor to use for a particular XRT data frame, the *xrtpipeline* performs a linear interpolation between the gain factors at each of the 3 specified temperatures to match the temperature of the data frame.

#### Update of CTI coefficients:

An updated analysis of the charge transfer inefficiency (CTI) coefficients has been performed using data collected in full-frame PC mode during 15 September, 2005.

#### 4. Scientific Impact of this Update:

The accuracy of XRT spectral feature positions should be significantly improved due to the incorporation of the temperature dependent gain information. The spectral resolution of features in datasets spanning wide temperature ranges will also be improved by the temperature dependent gain.

#### 5. Caveat Emptor:

It is noted that significant charge traps exist in certain columns (as indicated within the document text) of the XRT CCD which may cause the local effective gain to be markedly different from that described by the global gain/CTI coefficients contained in the released gain calibration files. The form of the Calibration Database does not currently allow for precise correction for such traps in the XRT standard processing tools (*xrtpipeline*). It is further noted that an apparent offset has been seen in selected WT data sets produced by *xrtpipeline* using these calibration products. The cause of this offset is

presently not fully understood and an investigation is ongoing.

## 6. Expected Updates:

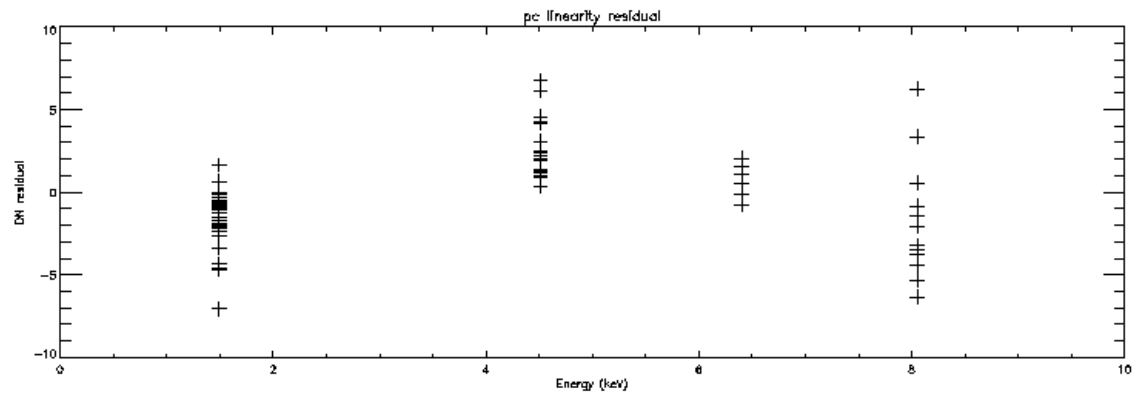
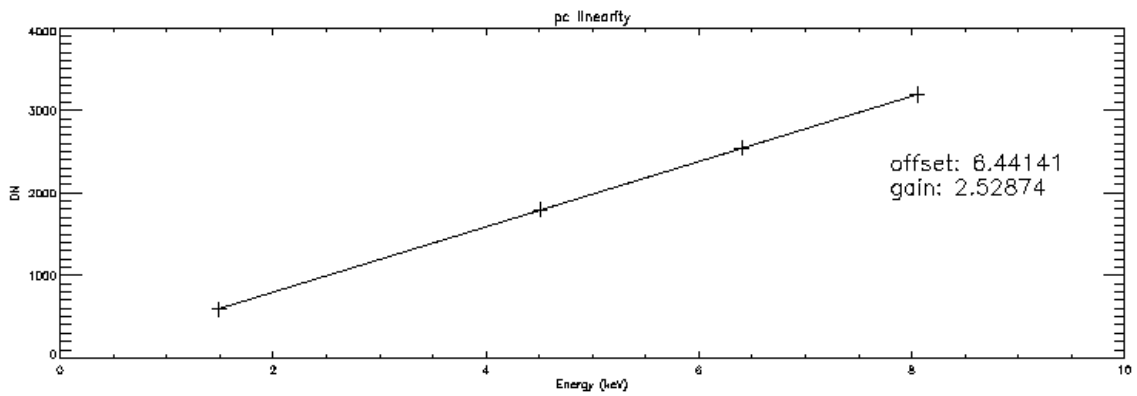
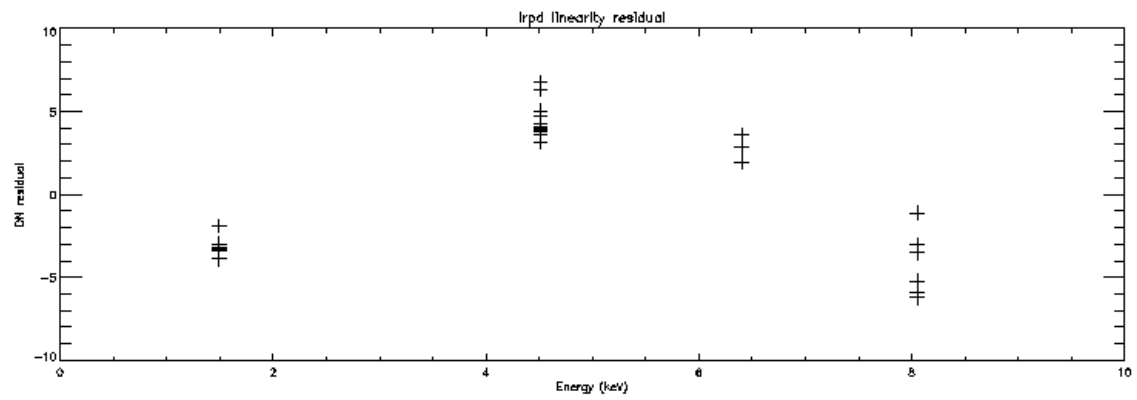
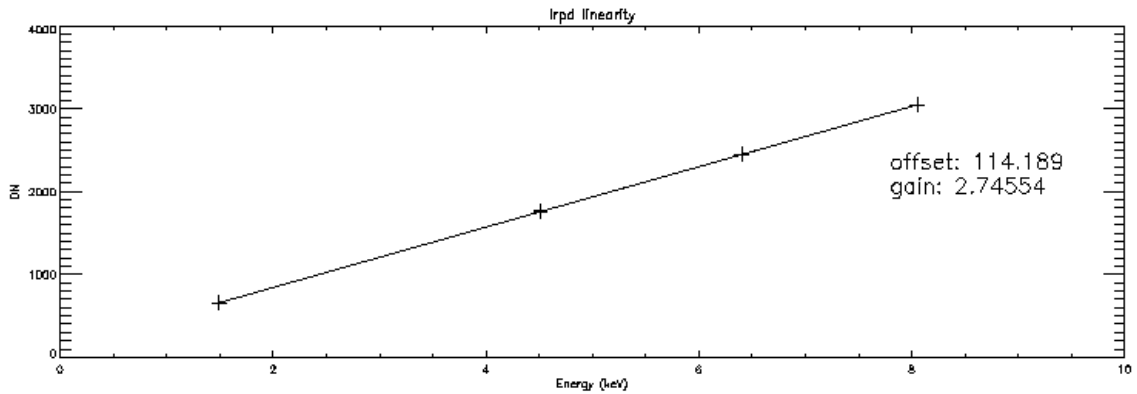
It is expected that radiation damage during the orbital lifetime of Swift will degrade the XRT CCD charge transfer efficiency through the production of more charge traps. Periodic updates to the gain files will be made to account for these changes.

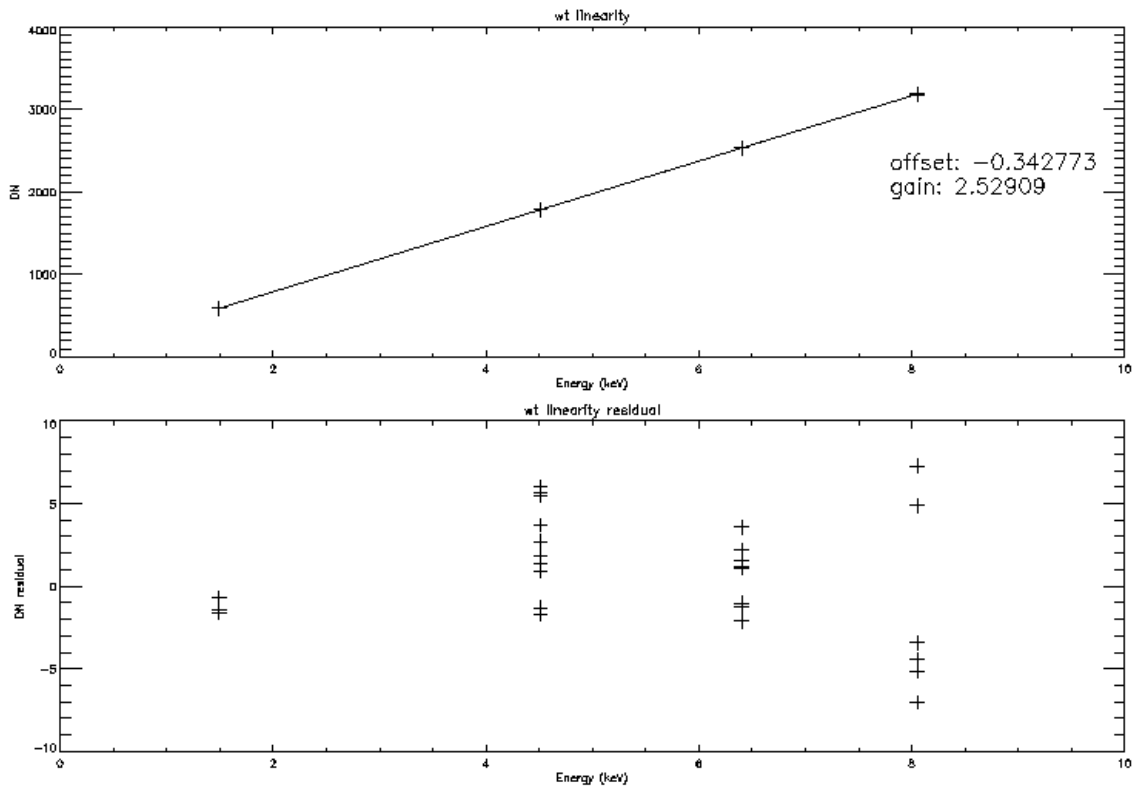
## 7. Panter Gain calibration:

The original gain calibration for the XRT in all modes was determined from data collected at the Panter X-ray calibration facility during Sept-Oct 2002 (with CCD temperature of  $-100$  C). The nominal gain factor in each mode has been determined by performing a linear fit of digital number (DN) to eV of discrete line data collected at energies of 1.49 keV (Al K<sub>α</sub>), 4.51 keV (Ti K<sub>α</sub>), 6.4 keV (Fe K<sub>α</sub>) and 8.05 keV (Cu K<sub>α</sub>). Data at 0.28 keV (C K<sub>α</sub>) were found to be contaminated by background and hence were not used in the calibration. Plots of the gain linearity (in DN vs energy for each mode) are displayed below together with the associated residual of the linear fit to the gain in each mode.

As the current format of the gain Calibration Database file does not support a polynomial description of the gain function, we have chosen to perform the gain calibration using the higher energy values, leaving the slight discrepancy at lower energies to be corrected in later versions of the ground/in-flight calibration. The nominal gain values determined as described above for each mode for the Panter calibration data are:

low rate photodiode: 2.75 eV/DN  
photon counting: 2.529 eV/DN  
windowed timing: 2.529 eV/DN





## 8. Thermal Vacuum Gain Calibration (LrPD):

One amendment to the above strategy has become necessary because the low-rate photodiode mode (LrPD) waveform was altered after the completion of the Panter calibration period, changing the value of the nominal gain for this mode. To recalibrate the LrPD mode gain, we have performed a linear fit to the Mn K<sub>α</sub> (5.993 keV doublet) and Mn K<sub>β</sub> (6.490 keV) lines collected in thermal vacuum testing during June 2004 (after the waveform change, with CCD temperature of  $-100$  C). The nominal gain values determined as described above for each mode are:

low rate photodiode: 2.55 eV/DN

photon counting: 2.529 eV/DN

windowed timing: 2.529 eV/DN

## 9. Temperature Dependent Gain Calibration Factor Analysis:

XRT gain calibration is performed in orbit using the well defined lines of the Cassiopeia

A supernova remnant (Holt et al 1994, PASJ, 46, L151). It was noted soon after first light that the warmer operating temperature regime caused a change in the XRT gain of  $\sim 2\%$ . Further analysis showed that the function of gain with temperature can be fit well by a simple linear relationship. Taking advantage of the wide range of temperatures at which data have been collected on Cas A together with measurements of the gain at  $-100^\circ\text{C}$  from ground testing, the XRT gain factor as a function of temperature has been derived. Each of the three XRT observing modes has been calibrated independently, though all are expected to yield similar results. Table 1 shows the dates and XRT CCD temperature ranges of observations used in the gain calibration analysis.

Observation Date	Min CCD_T (degrees C)	Max CCD_T (degrees C)
2004-346	-65	-49
2004-347	-55	-48
2004-358	-64	-47
2005-034	-57	-47
2005-035	-58	-47
2005-047	-65	-51
2005-048	-62	-58

Table: Observation dates and minimum/maximum XRT CCD temperature during the observations of Cassiopeia A data used to calibrate the *Swift* XRT gain in orbit.

The observations have been separated by CCD temperature, grouping the frames into one degree bins from  $-46\text{C}$  to  $-64\text{C}$ . Once each one-degree wide bin of frames had been collected, the resulting spectrum was grouped to have at least 20 counts per PI bin and then analyzed using the XSPECv11 software package to simultaneously fit all lines defined in Holt et. al. using a power-law model plus 14 Gaussian lines.

Once a best fit power law plus multiple Gaussian model was fit to each 1-degree wide data set, a linear fit of known line energy to observed digital number(DN) value was performed to determine the individual gain factor for the dataset at each temperature bin. To minimize the effect of the weaker, more crowded lines in the fit, the fit was performed iteratively, removing the 3-sigma outliers after each successive fit and refitting the remaining lines. Once a gain factor had been determined in this way for each of the 1-degree data sets, a linear function was then fit to the gain factors versus temperature. The fit of gain factor to temperature is weighted by the inverse of the uncertainty in each of the individual gain factors (as defined by the standard deviation of the data in each bin) and is performed iteratively, removing 3-sigma outliers.

This fitting technique produces a temperature dependent correction to the gain factor of  $0.00117 \text{ eV/DN}/^\circ\text{C}$ . If we extrapolate this function backwards from the fitted data to the ground calibration temperature of  $-100^\circ\text{C}$ , we see that this fit yields a slightly larger value

for the gain at  $-100^{\circ}\text{C}$  than the ground calibration value of  $2.529\text{ eV/DN}$  (the extrapolated value is  $2.537$ ). If we assume that the gain truly varies as a linear function across the entire temperature range  $-100^{\circ}\text{C}$  to  $-50^{\circ}\text{C}$ , then we may recompute our fit including the ground calibration value of the gain at  $-100^{\circ}\text{C}$  into our dataset. If we do this and refit the data as described before, the function of the gain factor with temperature becomes (see the figure below)  $0.00138\text{ eV/DN}^{\circ}\text{C}$ . Because we do not have evidence whether the gain does indeed vary linearly with temperature from  $-100^{\circ}$  to  $-50^{\circ}\text{C}$ , we have chosen to use the value of  $0.00117\text{ eV/DN}^{\circ}\text{C}$  to modify the Gain CALDB file as determined from on orbit data at operational temperatures.

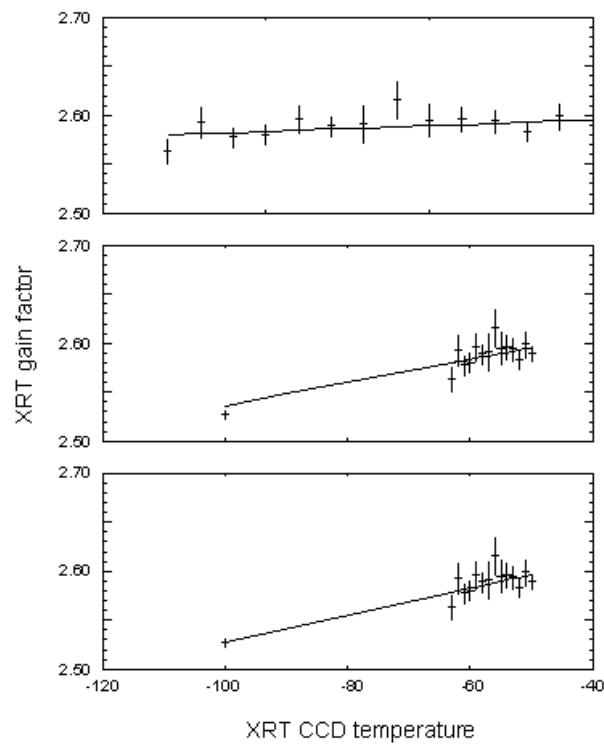


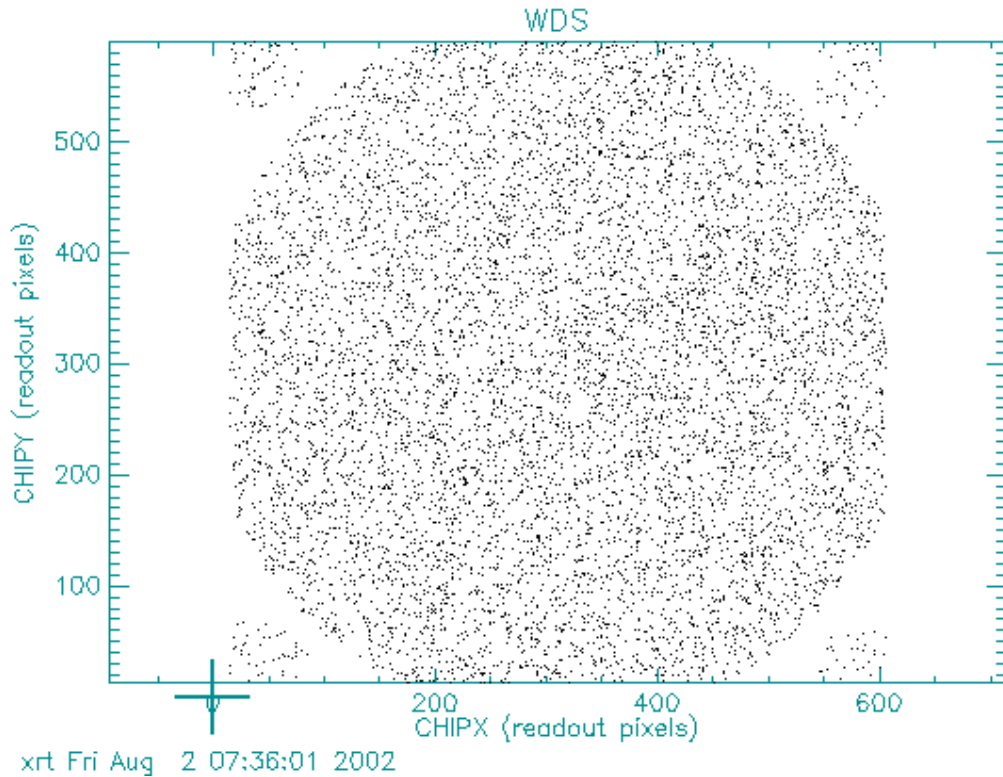
Figure: Fit of XRT gain factor versus XRT CCD temperature. The upper panel shows the fit performed only to the data collected in orbit on Cassiopeia A where the calculated gain correction value is  $0.00117\text{ eV/DN}^{\circ}\text{C}$ . The middle panel is the on-orbit fit extrapolated to the temperature at which ground calibration data was collected,  $-100^{\circ}\text{C}$ . The point plotted at  $-100^{\circ}\text{C}$  is the gain value determined during ground calibration of  $2.529\text{ eV/DN}$ . The lower panel shows the result of fitting for the gain versus temperature factor including all on-orbit data and the ground calibration data collected at  $-100^{\circ}\text{C}$ . The gain versus temperature correction factor using all data is  $0.00138\text{ eV/DN}^{\circ}\text{C}$ .

## 10. CTI Analysis:

### Pre-Launch Analysis:

The XRT CCD has 4  $^{55}\text{Fe}$  calibration sources mounted at the 4 corners of the detector for

in-flight calibration and monitoring. The decay of  $^{55}\text{Fe}$  to  $^{55}\text{Mn}$  in the calibration sources produces a doublet line (Mn  $K\alpha$ ) at 5.88 and 5.899 keV and a weaker, singlet line (Mn  $K\beta$ ) at 6.49 keV. In addition to the sources mounted on the CCD, an  $^{55}\text{Fe}$  source mounted on the back of the XRT focal plane camera door illuminates the focal plane while the door is in the closed position (that is, blocking the optical path). The regions of the detector illuminated by each source can be clearly seen in the figure below.



The CTI analysis is performed using Mn  $K_{\alpha}$  data from the thermal vacuum testing period (with CCD temperature of  $-100\text{ C}$ ). Approximately  $1.9 \times 10^6$  single pixel events have been selected from the output of the PSU *pass1* software from the following list of days/observations:

150_0355	150_0448	150_0719	150_1050
152_1658	153_0234	155_0351	158_1031
159_1935	160_0403	160_0500	160_0816
160_1956	160_2153	160_2327	161_0146

These events are composed both of corner source events (about  $1 \times 10^5$  events) and door source events (about  $1.8 \times 10^6$  events). We will henceforth define the XRT corner source configuration as follows:

```
DetX>
CS2  CS3
```

^

DetY

CS0 CS1

SERIAL REG

amp/

Following this numbering convention, the initial strategy for determining the global CTI coefficients for the detector is to measure the Gaussian centroid of the Mn K<sub>α</sub> events from each of the 4 corner sources, where we have defined a 50 pixel x 50 pixel square region at each corner of the detector to spatially select events. We then calculate the difference in the Gaussian centroids measured at CS0 and CS1 divided by the mean Detector X position as the fractional serial CTI coefficient (that is, the calibration file CTI coefficient times the photon DN value). The parallel CTI coefficient is measured analogously using the CS2-CS0 corner source pair and also using the CS3-CS1 pair.

The Gaussian centroids found for each individual corner source are shown below with 1-sigma gaussian line width (FWHM/2.35) shown in parentheses and estimated errors:

CS0: 2328.7 +/- 1 (22.5 +/- 1) DN

CS1: 2324.3 +/- 1 (23.1 +/- 1) DN

CS2: 2326.2 +/- 1 (22.8 +/- 1) DN

CS3: 2322.5 +/- 1 (23.7 +/- 1) DN

Using the strategy outlined above, these Gaussian centroid values lead to serial and parallel CTI measures of (errors estimated):

2-0 parallel:  $2.0 \times 10^{-6} \pm 2 \times 10^{-6}$

3-1 parallel:  $1.4 \times 10^{-6} \pm 2 \times 10^{-6}$

0-1 serial:  $3.4 \times 10^{-6} \pm 2 \times 10^{-6}$

Using the door source counts, though, we can investigate the parallel CTI in greater detail by actually mapping out the parallel CTI column by column.

We do so as follows:

Between columns 50 and 550 (roughly where the door source counts strike the CCD) each column of the detector receives about 3500 counts, evenly distributed among the 600 pixels in the column. Below column 50 and above column 550 where primarily corner source counts reach the detector, we have only about 1000 counts per column. We do a simple least squares linear fit to all the events in each column (one column at a time).

We expect the CTI coefficient found for each individual column using this method to be similar to the coefficients noted above found using only the corner sources, with possible exceptions due to traps in individual columns. The overall average of the CTI coefficients found for each column using this method (average of 596 individual columns since the use of single pixel events excludes columns 1-2 and columns 599-600 from this analysis) is  $1.6 \times 10^{-6}$ , in good agreement with the average value found from the 2 parallel pairs of corner sources of  $1.7 \times 10^{-6}$  (average of  $1.4 \times 10^{-6}$  and  $2.0 \times 10^{-6}$ ).

We additionally note, however, that there are 6 columns containing significant charge traps; Detector X coord columns: 54, 78, 110, 140, 259, 294. The traps found in columns are demonstrated below in plots of (DN vs row) for each column considered to contain a charge trap. The left plot in each pair shows all events in the column plotted as individual points while the right plot show only the median DN value recorded in each (row) pixel of the column. The top of the left plot in each pair is labeled with the Detector X position column number and the derived parallel CTI coefficient for that column.

If we exclude these 6 columns from the average of all column CTI coefficients we did earlier, we find an overall parallel CTI average coefficient of  $1.4 \times 10^{-6}$ , now using 590 columns rather than 596 as before.

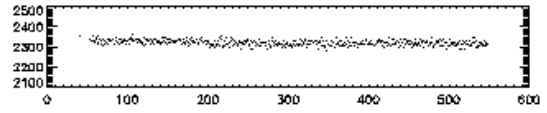
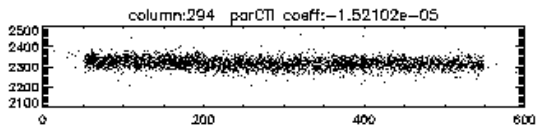
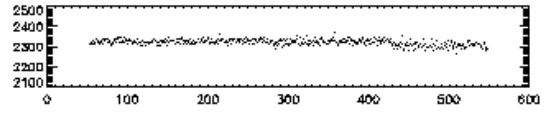
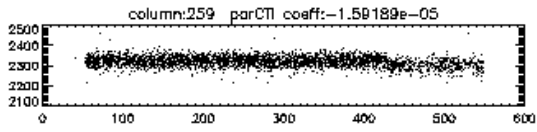
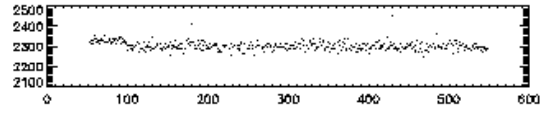
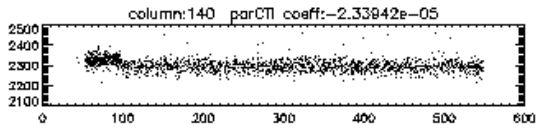
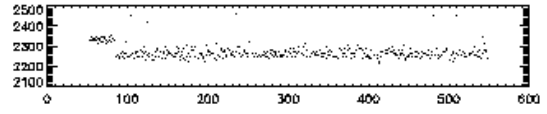
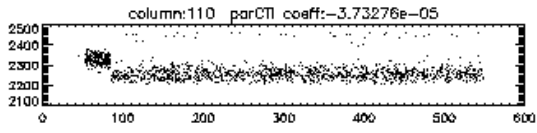
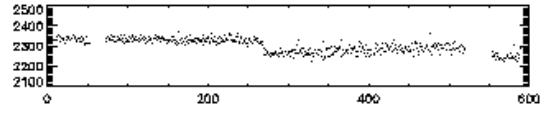
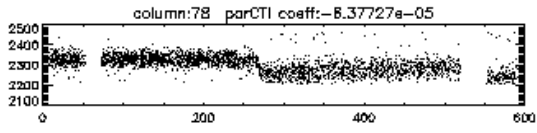
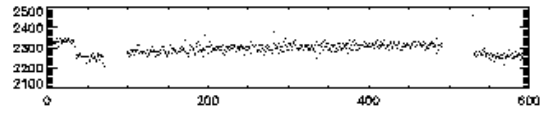
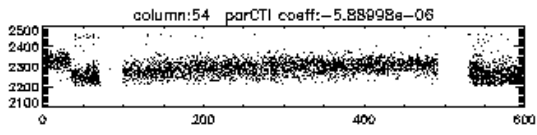
Shown in the second figure below we present (from top to bottom)

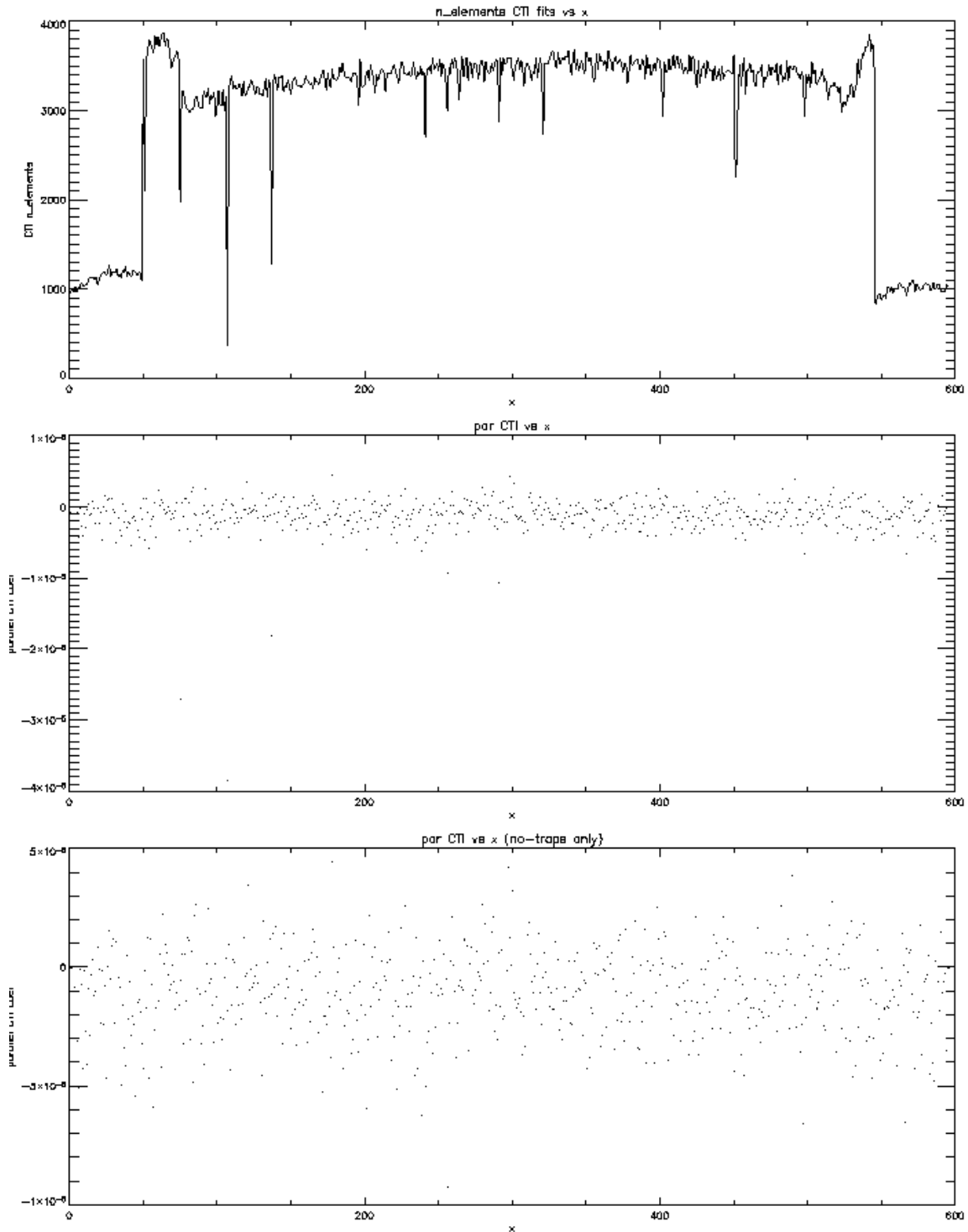
1. a figure of (number of events) vs (column number) showing that most columns are fit using more than 3000 events and that no column is fit using fewer than 1000 events
2. a plot of the parallel CTI coefficient determined from the individual column fits vs column number. 5 of the 6 columns containing charge traps are clearly identifiable in the figure by the CTI coefficient below  $-1 \times 10^{-5}$  while the 6<sup>th</sup> trapped column (column 54) oddly fits best to a moderate CTI value of  $-6 \times 10^{-6}$ , though a trap clearly exists (from the plot of DN vs column)
3. an expanded view of the CTI coefficient vs column number, where we have shown only the columns believed to not contain a trap.

Given this analysis, we have uploaded gain calibration files (Cal Version 003) to the SDC using the following CTI coefficients:

**serial CTI:  $3.4 \times 10^{-6}$**

**parallel CTI:  $1.4 \times 10^{-6}$  (the average across the detector)**





### On-Orbit Analysis (Sept 15, 2005):

During the first 9 months of the mission, data from the corner sources was unavailable due to telemetry bandwidth constraints. In September 2005, corner source data was collected which was then used to perform an updated CTI analysis. Using the

nomenclature and method defined above, we find Gaussian centroids for each individual corner source as shown below; 1-sigma gaussian line width (FWHM/2.35) shown in parentheses and estimated errors:

CS0: 2264 +/- 1 (29.1 +/- 1) DN

CS1: 2253 +/- 1 (29.9 +/- 1) DN

CS2: 2280 +/- 1 (26.3 +/- 1) DN

CS3: 2272 +/- 1 (27.4 +/- 1) DN

yielding CTI measures of (estimated errors):

parallel (2-0) :  $1.3 \times 10^{-5} \pm 2 \times 10^{-6}$

parallel (3-1) :  $1.5 \times 10^{-5} \pm 2 \times 10^{-6}$

serial (0-1) :  $6.5 \times 10^{-6} \pm 2 \times 10^{-6}$

Using this updated analysis, a new set of CTI coefficients has been appended to the Gain CALDB file which will be used to calibrate data collected after September 1, 2005:

**serial CTI:  $6.5 \times 10^{-6}$**

**parallel CTI:  $1.4 \times 10^{-5}$  (the average across the detector)**

Data taken previously to September 1, 2005 will continue to be calibrated using the CTI coefficients defined earlier in the document, which remain in the CALDB gain file to be applied to data collected early in the mission as appropriate.